

## THE EXTREME SOLAR STORMS OF OCTOBER TO NOVEMBER 2003

S.P. Plunkett  
Space Science Division

### AN OVERVIEW OF SOLAR ACTIVITY AND SPACE WEATHER

In recent decades, humans have come to rely on space technology for an ever-increasing variety of purposes, including human exploration of the solar system, scientific research, national defense, and commercial activities. The field of space weather seeks to understand and predict variability in the space environment.<sup>1</sup> The Sun is the source of all space weather, and the origins of major space weather storms can be traced to explosive releases of magnetic energy from the solar atmosphere in the form of solar flares and coronal mass ejections (CMEs). A solar flare occurs when a sudden release of energy in an active region of the solar atmosphere leads to rapid heating of a localized region of the atmosphere, and rapid acceleration of charged particles to relativistic energies. A CME involves the expulsion of large amounts of ionized plasma and magnetic field from the Sun into interplanetary space (Fig. 1). A typical CME involves the ejection of about  $10^{13}$  kg of plasma, at speeds from a few hundred km/s up to a few thousand km/s, into interplanetary space. A major scientific objective of contemporary research in solar-terrestrial physics is to understand how and why these events occur on the Sun, and how to predict their occurrence and their effects on humans in space and on technological systems both in space and on the ground.

#### Impact of Space Weather

The potential impacts of space weather are numerous. Spacecraft and the instruments they carry can suffer adverse effects from direct particle bombardment or electrostatic discharge, ranging from temporary anomalies to complete failure of critical systems. Humans living and working in space can receive radiation doses well in excess of recommended limits. Star trackers that are frequently used to orient spacecraft can lose their ability to lock on to patterns in the background stars when high energy particles strike

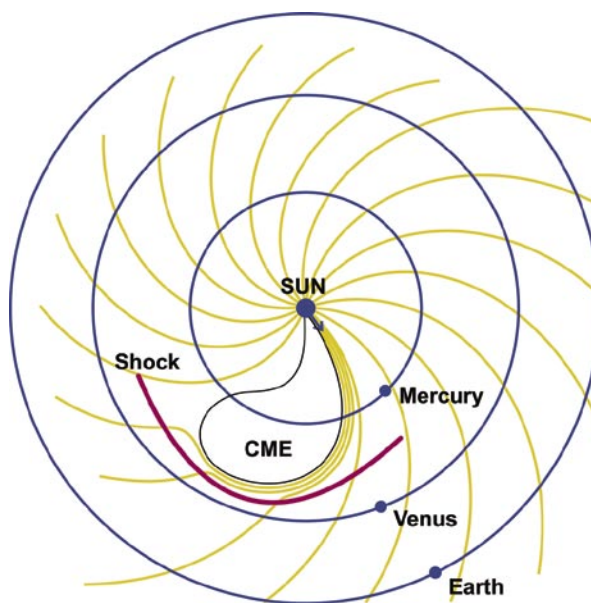


**FIGURE 1**  
Sketch of the inner heliosphere, showing the spiral shape of the interplanetary magnetic field caused by solar rotation, and a CME driving a shock as it propagates outward from the Sun.

their detectors, thus causing spacecraft to lose attitude control. The impact of a CME on the Earth's environment can lead, under the right circumstances, to severe worldwide disturbances of the terrestrial magnetic field known as geomagnetic storms. The resulting particle acceleration and heating of the upper atmosphere can lead to increased drag on satellites in low Earth orbit, causing their orbits to change unpredictably. The ionosphere is usually disturbed during a geomagnetic storm, leading to difficulties with both terrestrial and satellite-borne communications systems that either transmit radio signals through the ionosphere or use it to "bounce" signals over large distances. For example, Global Positioning System (GPS) operations are affected by fluctuations in the total electron content (TEC) of the ionosphere along the path to the satellite. Spacecraft that use the Earth's magnetic field for guidance can lose orientation during a geomagnetic storm. At ground level, fluctuations in the magnetic

Report Documentation Page				Form Approved OMB No. 0704-0188	
Public reporting burden for the collection of information is estimated to average 1 hour per response, including the time for reviewing instructions, searching existing data sources, gathering and maintaining the data needed, and completing and reviewing the collection of information. Send comments regarding this burden estimate or any other aspect of this collection of information, including suggestions for reducing this burden, to Washington Headquarters Services, Directorate for Information Operations and Reports, 1215 Jefferson Davis Highway, Suite 1204, Arlington VA 22202-4302. Respondents should be aware that notwithstanding any other provision of law, no person shall be subject to a penalty for failing to comply with a collection of information if it does not display a currently valid OMB control number.					
1. REPORT DATE <b>2005</b>		2. REPORT TYPE		3. DATES COVERED <b>00-00-2005 to 00-00-2005</b>	
4. TITLE AND SUBTITLE <b>The Extreme Solar Storms of October to November 2003</b>				5a. CONTRACT NUMBER	
				5b. GRANT NUMBER	
				5c. PROGRAM ELEMENT NUMBER	
6. AUTHOR(S)				5d. PROJECT NUMBER	
				5e. TASK NUMBER	
				5f. WORK UNIT NUMBER	
7. PERFORMING ORGANIZATION NAME(S) AND ADDRESS(ES) <b>Naval Research Laboratory, Space Science Division, 4555 Overlook Ave. S.W., Washington, DC, 20375</b>				8. PERFORMING ORGANIZATION REPORT NUMBER	
9. SPONSORING/MONITORING AGENCY NAME(S) AND ADDRESS(ES)				10. SPONSOR/MONITOR'S ACRONYM(S)	
				11. SPONSOR/MONITOR'S REPORT NUMBER(S)	
12. DISTRIBUTION/AVAILABILITY STATEMENT <b>Approved for public release; distribution unlimited</b>					
13. SUPPLEMENTARY NOTES					
14. ABSTRACT					
15. SUBJECT TERMS					
16. SECURITY CLASSIFICATION OF:			17. LIMITATION OF ABSTRACT <b>Same as Report (SAR)</b>	18. NUMBER OF PAGES <b>8</b>	19a. NAME OF RESPONSIBLE PERSON
a. REPORT <b>unclassified</b>	b. ABSTRACT <b>unclassified</b>	c. THIS PAGE <b>unclassified</b>			

field can induce significant currents (sometimes over 100 amps) to flow in long-distance pipelines and transmission lines for electrical power, leading to brownouts and blackouts and damage to expensive transformer equipment. The most famous example of this occurred in 1989, when a geomagnetic storm led to a failure of the electrical grid across the north-eastern United States and Canada. The intense particle acceleration can also lead to beautiful auroral displays at much lower latitudes than the polar regions of the Earth where this phenomenon is usually visible.

The National Oceanic and Atmospheric Administration (NOAA) monitors and forecasts space weather for civilian purposes in the United States. NOAA has developed a set of space weather scales as a way to describe the environmental disturbances and potential impacts of geomagnetic storms, solar particle storms, and radio blackouts. The scales have numbered levels, ranging from 1 for the least severe events to 5 for the most severe events, and are analogous to the well-known scales used in terrestrial meteorology to classify hurricanes, tornadoes, and earthquakes.

## OBSERVING THE SUN FROM SPACE: THE SOHO MISSION

The Solar and Heliospheric Observatory (SOHO)<sup>2</sup> observes the Sun continuously from an

orbit around the L1 Lagrange point, located approximately 1% of the distance along an imaginary line from the Earth to the Sun (Fig. 2). SOHO is a joint mission of the European Space Agency (ESA) and the National Aeronautics and Space Administration (NASA) and has been operating almost continuously since launch in December 1995. SOHO carries 12 scientific instruments, including two in which NRL plays key roles. The first of these is the Large Angle Spectrometric Coronagraph (LASCO), a suite of telescopes that observes the outer atmosphere of the Sun (the solar corona) in visible light over a range of altitudes from  $2 R_{\odot}$  to  $30 R_{\odot}$  from the center of the solar disk ( $1 R_{\odot} = 6.96 \times 10^5$  km, the radius of the Sun). This is accomplished by using an opaque occulting mask assembly in front of the telescope objective to block direct solar light, thus allowing the faint corona to be observed. White-light coronagraphs, such as LASCO, detect light that is Thomson-scattered off free electrons in the highly ionized corona. The principal investigator for LASCO is Dr. Russell Howard of the NRL Solar Physics branch. The second NRL instrument on SOHO is the Extreme Ultraviolet Imaging Telescope (EIT). EIT images the corona directly above the solar disk in four wavelengths in the extreme ultraviolet (EUV) region of the spectrum, corresponding to emission lines from coronal ions with peak emissivity at temperatures ranging from  $5 \times 10^4$  K to  $2 \times 10^6$  K.

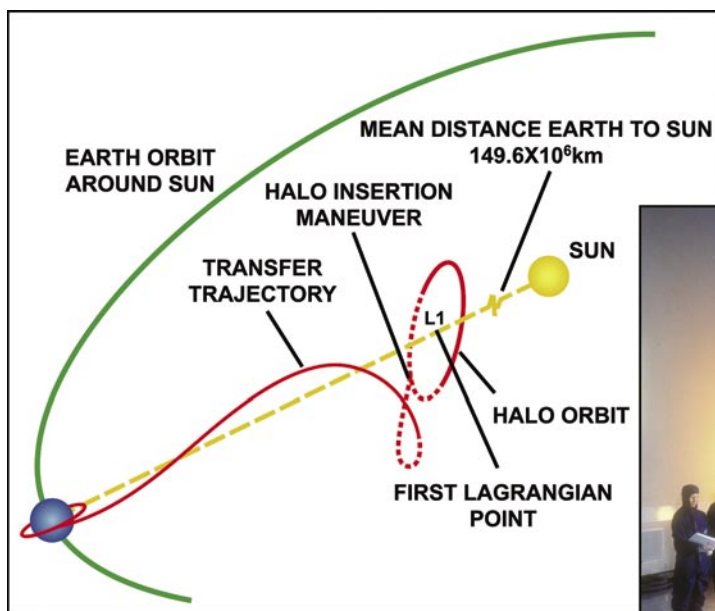
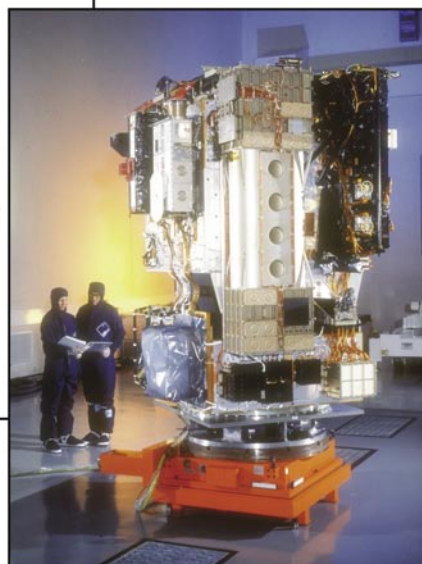


**FIGURE 2**

The SOHO spacecraft (right) and its halo orbit about the L1 point between the Earth and the Sun (left). The black box on the upper right of the spacecraft is the LASCO instrument. The EIT instrument is not visible in this view.



LASCO and EIT share common resources on the SOHO spacecraft, and together they provide a comprehensive view of activity in the corona.

## HALLOWEEN FIREWORKS: THE EVENTS OF OCTOBER TO NOVEMBER 2003

Solar activity waxes and wanes with a periodicity of approximately eleven years (Fig. 3). At the peak of solar activity, known as solar maximum, about 5 CMEs/day occur from all regions of the solar disk. At solar minimum, the rate is only about 0.6 CMEs/day, mostly near the solar equator. The current solar cycle peaked in late 2000, and solar activity has generally been decreasing since about that time. In early October 2003, however, solar observers working with data from the SOHO mission were surprised to see evidence of unusually high levels of activity on the far side of the Sun. The Sun rotates on its axis with a period of 27 days at the equator, and on October 18, a large active region rotated into view just north of the equator, designated as NOAA active region (AR) 484. On October 22, AR 486 appeared on the east limb, about 15° south of the equator, and on October 27, AR 488 emerged close to disk center and about 10° north of the equator. From October 19 through November 4, these regions produced a combined total of 12 X-class flares, including two of the largest flares ever observed, along with numerous smaller M-class and C-class flares (Fig. 4). Solar flares are classified according to their peak X-ray flux. The brightest (and least common) flares are X-class flares, with peak X-ray flux above  $10^{-4}$  W/m<sup>2</sup>. M-class flares have one-tenth of the flux in X-class flares, and C-class flares have one-tenth of the flux in M-class flares. The X-flares in this period were all accompanied by large, energetic CMEs. The masses and kinetic energies of the CMEs

were measured from LASCO images. The masses are in the top 5% and the kinetic energies are in the top 1% of all CMEs observed by LASCO over almost 9 years of operation.

## OCTOBER 28 AND 29, 2003 SOLAR ERUPTIONS

On October 28, AR 486 was located close to the sub-Earth point on the solar disk, at 8° east of central meridian longitude, and 16° south in latitude (Fig. 5). It had developed into the largest active region of the current solar cycle, and had a highly complex appearance indicating a substantial amount of free energy in the magnetic field. At 11:10 UTC on that day, AR 486 produced one of the largest flares of this solar cycle, and the fourth largest flare ever recorded. This flare was classified as X17 (peak X-ray flux of  $1.7 \times 10^{-3}$  W/m<sup>2</sup>). The event also produced a category R4 (severe) radio blackout on Earth. An extremely fast CME moving at an apparent speed of almost 2,500 km/s was observed in LASCO imagery. Since a coronagraph shows features projected onto a plane extending above the limb of the Sun at a right angle to the line of sight (the “plane of the sky”), this measured speed is a lower limit to the true speed of the CME. The mass of the CME was estimated to be in the range  $1.4$  to  $2.1 \times 10^{13}$  kg, yielding a kinetic energy in the range  $4.2$  to  $6.4 \times 10^{25}$  J. This is one of the most energetic CMEs observed by LASCO. The CME appeared as a bright ring surrounding the occulting disk that is used to block out the Sun’s disk in the LASCO coronagraphs. Events like this are called “halo” CMEs, and they are indicative of material ejected along the line between the Sun and the Earth. A thin, sharp ring of emission was observed ahead of the CME, extending all the way around the occulting disk. This is identi-

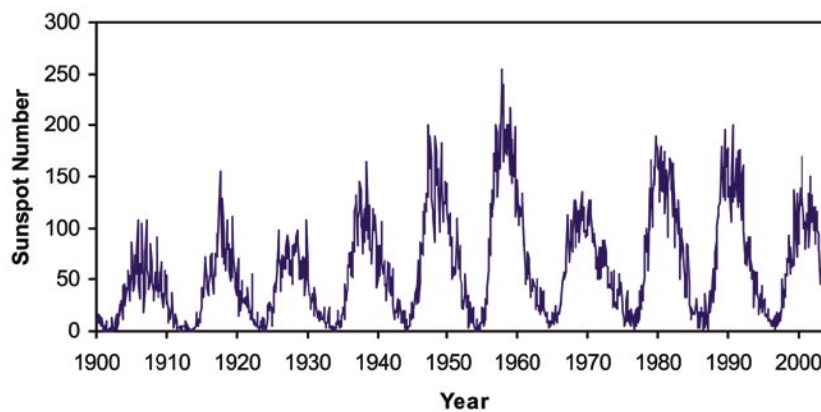


**FIGURE 3**

The monthly-averaged number of sunspots visible on the surface of the Sun since 1900. The number of spots and the associated level of solar activity vary with a period of about 11 years.



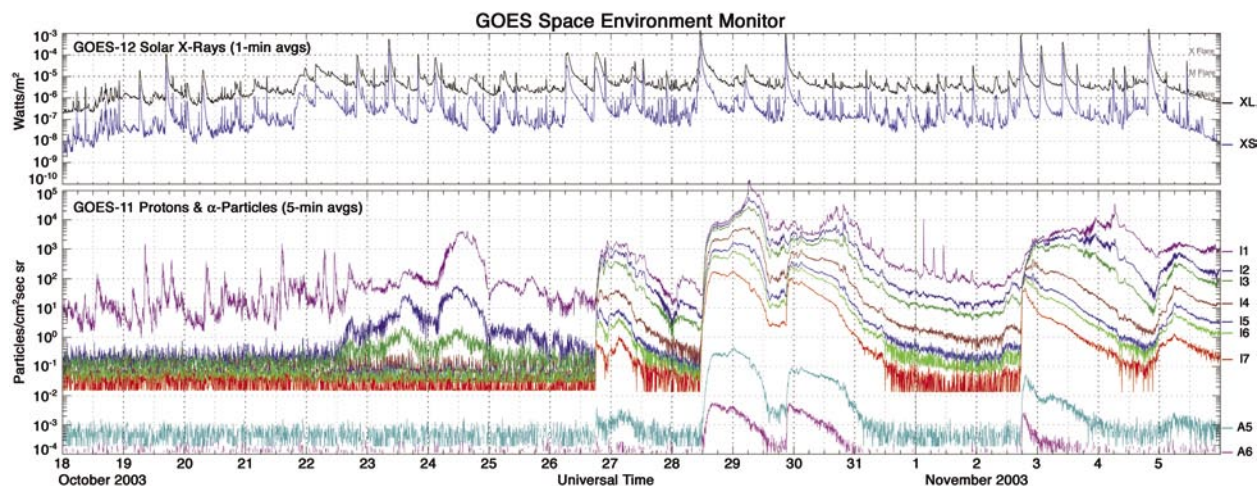


**FIGURE 4**

Solar X-ray and energetic particle fluxes measured by instruments on the NOAA GOES spacecraft from October 18 to November 5, 2003. The top panel shows the X-ray flux in two wavelength bands (1 to 8 Å in black, 0.5 to 3 Å in blue). Flares are identified as large, transient increases in the X-ray flux, with flare classes indicated on the right. The bottom panel shows protons in seven energy bands from >1 MeV to >100 MeV (traces labeled I1 to I7), and α-particles from 150-250 MeV (labeled A5) and 300-500 MeV (labeled A6).

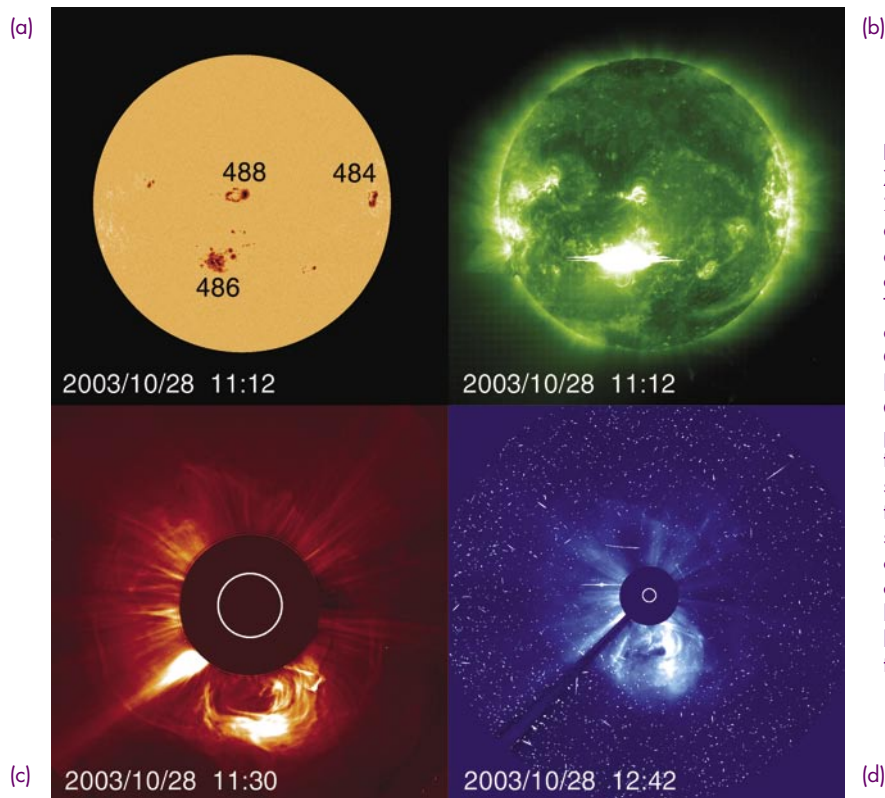


**FIGURE 5**

X17 flare and CME on October 28, 2003. (a) Shows active regions that are visible as dark spots on the image of the Sun from the SOHO Michelson Doppler Imager (MDI). (b) The EIT image of the corona shows a bright flare in AR 486. (c) LASCO C2 and (d) C3 images show a fast halo CME. The bright specks in the C3 image are caused by energetic particles striking the camera during the exposure. The location and size of the Sun are indicated by the white circle, and the filled circle surrounding the Sun is the portion of the image that is blocked by the coronagraph occulting mask. The lower left portion of the C3 image is blocked by the mechanical structure that supports the occulter.

fied as a shock front created as the fast-moving CME plows into the ambient corona and solar wind ahead of it. When LASCO observers noted this event in the images arriving at the SOHO operations center, they immediately alerted the NOAA Space Environment Center that an event with potentially significant space weather consequences was headed towards Earth.

On the following day, October 29, AR 486 produced another major eruption. An X10 flare (peak X-ray flux  $10^{-3}$  W/m<sup>2</sup>) occurred at 20:49 UTC, resulting in a class R4 (severe) radio blackout at Earth. Associated with this flare was another extremely fast Earth-directed halo CME, with a measured speed just over 2,000 km/s, and a kinetic energy of  $5.7 \times 10^{25}$  J.

### Particle Storm Reaches Earth Orbit

Following the CME and flare eruptions on October 28, an intense energetic particle event was observed in Earth orbit beginning around 11:50 UTC. Strong enhancements of the flux of both >10 MeV and >100 MeV protons were observed by the GOES spacecraft (1 eV =  $1.6 \times 10^{-19}$  J). The particle storm quickly reached a level of S3 (strong) on the NOAA space weather scales, and at its peak reached a level of S4 (severe), making it one of the largest of the current solar cycle, and the fourth largest particle storm since records began in 1976. An event of this magnitude is sufficient to cause passengers and crew on high-flying aircraft to receive a radiation dose approximately equivalent to one chest X-ray. As can be seen in Fig. 4, the particle event began with a very rapid increase in the flux of both protons and  $\alpha$ -particles within a short period of time across a wide range of energies. The particle flux reached a maximum early on October 29, with the peak flux at lower energies occurring several hours later than at the highest energies. The flux then decayed slowly over the next several days, with a secondary enhancement late on October 29 following the X10 flare and CME from the same active region. The particle storm from the October 29 event reached a level of S3 (strong). The time profile of this combined particle event is typical of that expected if the particles are accelerated by a shock wave driven by a CME originating near central meridian longitude on the solar disk. The shock from the event on October 28 was detected at the L1 point by the Advanced Composition Explorer (ACE) spacecraft at 05:59 UTC on October 29, and it reached Earth at 06:13 UTC. The transit time for this CME from Sun to Earth was about 19 hours, making it one of the fastest on record. The CME on October 29 also traveled to Earth in about 19 hours, with the shock impacting the

Earth's magnetosphere around 16:00 UTC on October 30. A typical CME takes about three days to travel this distance, and the fastest on record took about 15 hours in August 1972.

### Solar Eruption Impact

Geomagnetic activity associated with the impact of these shocks and CMEs on the Earth's magnetosphere reached extreme levels. The arrival of the shock on October 29 triggered an abrupt perturbation of the Earth's magnetic field known as a "sudden commencement." This was followed by a category G5 (extreme) geomagnetic storm that lasted for 27 hours and was the sixth most intense storm on record (since 1932). Another G5 (extreme) geomagnetic storm resulted from the impact of the second shock and CME on October 30. Figure 6 shows the estimated planetary K index (Kp) for the three-day interval from October 29 to October 31. This index is a quasi-logarithmic measure of geomagnetic activity on a global scale, based on local measurements from a number of stations around the world, and updated every three hours. Values above Kp = 5, shown in red on the plot, indicate geomagnetic storm conditions. Values of Kp = 9 correspond to extreme storm conditions. Bright, colorful displays of the aurora, normally only visible from near-polar latitudes, were observed and photographed as far south as Florida on the nights of October 29 and 30.

### NOVEMBER 4, 2003 SOLAR ERUPTION

By early November, AR 486 had rotated close to the west limb as viewed from Earth and was about to disappear from view onto the far side of the Sun. On November 4, AR 486 was located right on the limb, at 89° west of central meridian longitude, and the visible disk was devoid of any significant active regions (Fig. 7). Just as solar observers were about to breathe a sigh of relief, and activity appeared ready to return to normal levels, AR 486 produced the largest X-ray flare ever recorded, at 19:31 UTC on November 4. The flare saturated the GOES X-ray detector, and later analysis yielded a peak X-ray flux at the X28 level (peak flux of  $2.8 \times 10^{-3}$  W/m<sup>2</sup>). Intense radio bursts across a broad range of frequencies were associated with the X28 flare. A category R5 (extreme) radio blackout resulted at Earth shortly after the flare. LASCO recorded an extremely fast CME, moving outward at a speed of 2,657 km/s. The mass of this CME was about  $1.5 \times 10^{13}$  kg, yielding a kinetic energy of  $5.3 \times 10^{25}$  J. Unlike the events of October

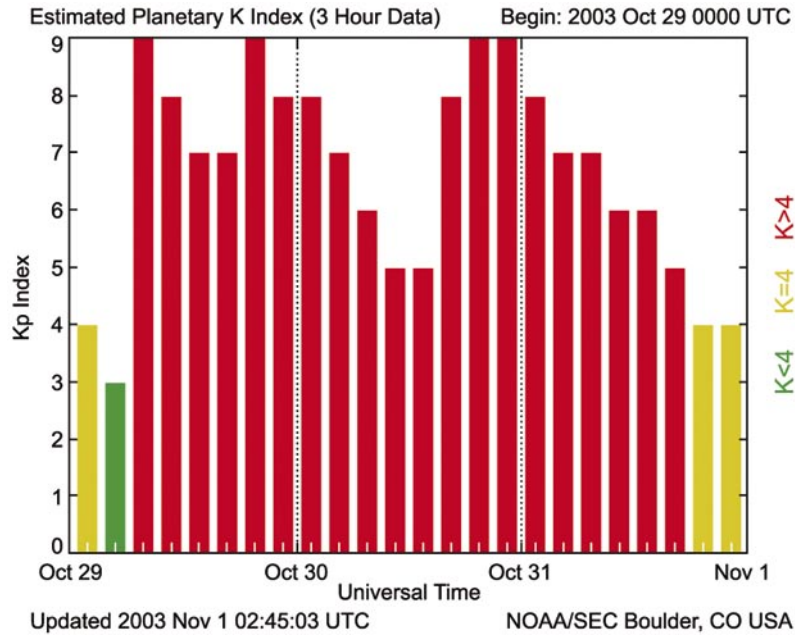


**FIGURE 6**

Geomagnetic Kp index from October 29 to October 31, 2003, showing severe storming in red.

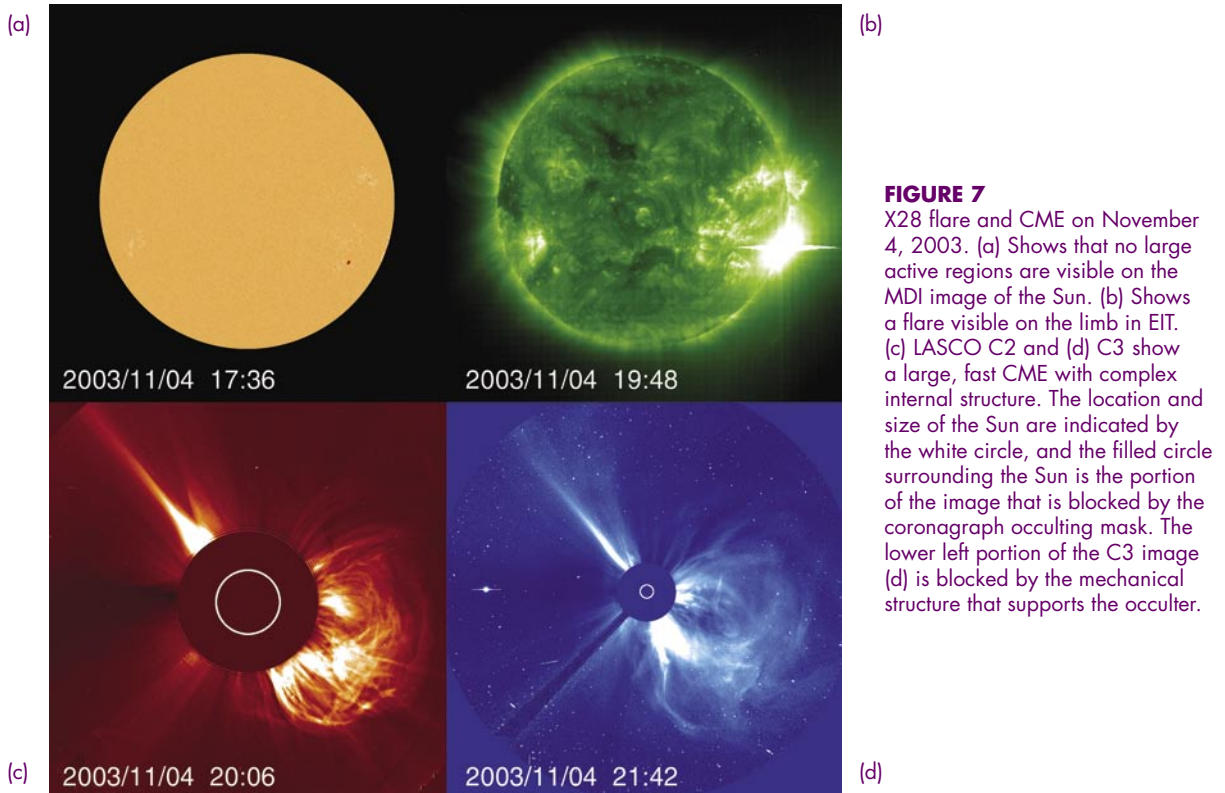


**FIGURE 7**

X28 flare and CME on November 4, 2003. (a) Shows that no large active regions are visible on the MDI image of the Sun. (b) Shows a flare visible on the limb in EIT. (c) LASCO C2 and (d) C3 show a large, fast CME with complex internal structure. The location and size of the Sun are indicated by the white circle, and the filled circle surrounding the Sun is the portion of the image that is blocked by the coronagraph occulting mask. The lower left portion of the C3 image (d) is blocked by the mechanical structure that supports the occulter.



28 and 29, in which the CMEs were observed almost head-on, this CME was observed edge-on, at almost 90° to the direction of propagation.

The particle flux in Earth orbit was already enhanced on November 4 due to an X8 flare and associated CME on November 2 (Fig. 4). As the particle flux was decaying, an enhancement in >10 MeV protons due to the X28 flare and associated CME was observed by GOES beginning at 22:25 UTC on November 4 (a much smaller enhancement was observed in >100 MeV protons). Although the flare occurred on the west limb, and the CME was not directed towards Earth, the particles were able to propagate to Earth because of the wide extent of the CME-driven shock and because the magnetic field lines along which the particles are constrained to travel form a spiral pattern connecting Earth to a solar longitude approximately 60° west of central meridian (Fig. 1). The particle flux rose gradually, with the >10 MeV proton flux peaking at 06:00 UTC on November 5, and then decayed slowly throughout the rest of that day. This time profile is typical of a particle event due to a CME-driven shock where the nose of the shock propagates well to the west of the observer, as was the case here. Because only the flank of the CME-driven shock propagated towards Earth, the shock was detected at L1 by the ACE spacecraft much later, around 19:00 UTC on November 6. For the same reason, despite the record size of the flare, and the large, fast CME, the particle storm at Earth only reached S2 (moderate) levels, and geomagnetic activity reached only a G1 (minor) storm level.

## IMPACTS ON TECHNOLOGICAL SYSTEMS

Near-Earth and deep space satellites and space operations, communications and navigation systems, the airline industry, and electric utilities were adversely impacted by the high levels of solar and geomagnetic activity during this period. Other systems were able to modify their operations to mitigate potential effects, and still others were able to continue normal operations based on real-time data and space weather forecasts. The detailed solar imagery available from the LASCO and EIT instruments was invaluable to NOAA space weather forecasters in making the predictions that enabled operators to take appropriate measures to protect their systems.

Numerous NASA missions were impacted by the October-November activity. The crew on the International Space Station (ISS) was directed to relocate to a shielded location on the station on at least five separate occasions to avoid radiation hazards. The robotic arm

on the ISS was powered down to protect it from possible radiation damage. The Martian Radiation Environment Experiment (MARIE) on the Mars Odyssey mission had a high temperature alarm on October 28 and was powered off. This instrument was not recovered. Contact with the Japanese Advanced Earth Observing Satellite II (ADEOS-2) was lost during a severe geomagnetic storm on October 24, caused by a CME associated with an X5 flare early on October 23. The ADEOS-2 payload included the \$150 million NASA SeaWinds instrument, a microwave radar experiment designed to map ocean wind speeds and directions. Several other NASA spacecraft had to use backup systems for attitude control during the particle storms, when star trackers were temporarily rendered unusable by the large number of particle hits. Other spacecraft switched into safe modes and turned off instruments during the periods of increased activity.

Airlines and ground controllers experienced communications difficulties almost daily in late October and early November, with the most severe problems occurring on polar routes between North America and Asia. At least one major airline rerouted polar flights to a route with better satellite communications links. Another major concern for airlines during this period was the potential impact of increased radiation levels on passengers and crew. On October 28, the Federal Aviation Administration (FAA) issued their first ever advisory warning that flights traveling at latitudes greater than 35° were subject to excessive radiation doses. Both major U.S. airlines that operate over the pole rerouted flights to nonpolar routes in response to this advisory notice, thus significantly increasing operating costs and time for these flights. Flights between the United States and Europe flew at lower than normal altitudes during this period. The FAA's Wide Area Augmentation System (WAAS), which uses GPS for aircraft navigation, was seriously impacted during the severe storms on October 29 and 30, and resulted in commercial aircraft being unable to use the WAAS for precision approaches.

Electric utilities in North America experienced minimal disruption, partly because of preventive measures taken to counter the effects of induced currents on the power grid based on space weather forecasts. More significant impacts occurred in Europe, and a power system failure occurred in Malmo, Sweden, on October 30, resulting in a city-wide blackout.

## LESSONS LEARNED

The observations presented here would not have been possible in any previous solar cycle. We now



have available a fleet of spacecraft with advanced instrumentation that allows us to observe an eruption on the surface of the Sun, and track that eruption all the way from the Sun to the Earth. We also have the tools to forecast with reasonable accuracy the potential space weather impacts of an eruptive event. We can identify solar active regions that are likely to produce large flares and CMEs, and we know that these events are powered by the conversion of free energy stored in magnetic fields on the Sun. However, we still do not know the details of the underlying mechanism that triggers these eruptive events, and we lack the ability to reliably predict when they will occur, so that accurately forecasting space weather more than a few days in advance is not possible. Future progress on this issue will require close synergy between observations and theoretical modeling using advanced computing techniques.

The NASA Solar-Terrestrial Relations Observatory (STEREO) mission will be launched in 2006. This mission will consist of two nearly identical spacecraft along the Earth's orbit. One spacecraft will lead, the other will lag behind the Earth, and both will drift apart at a rate of about 22° per year. NRL is leading a consortium that will provide identical suites of imaging instruments for both STEREO spacecraft, as well as theoretical modeling and data analysis efforts. The Sun-Earth Connections Coronal and Heliospheric Investigation (SECCHI) will obtain unprecedented stereoscopic views of the Sun and the heliosphere to a distance beyond the Earth's orbit. This will allow three-dimensional imaging of CMEs from their origin at the Sun to their impact on Earth, and will substantially increase our understanding of the structure and dynamics of CMEs and our ability to predict

space weather. STEREO will also allow us to view Earth-directed CMEs edge-on for the first time, thus revealing the detailed internal structure that is hidden in a head-on view. Some of the keys to understanding the potential space weather impacts of a CME, such as the topology of the magnetic field, lie in knowing these details about the internal structure. The edge-on view will also allow us to more accurately measure key parameters, such as the speed and mass of CMEs, that are difficult to determine from an end-on view.

In summary, the dramatic events of October and November 2003 demonstrate that our ability to observe and predict solar activity and its impact on technological systems in space and on the ground has improved dramatically in recent years. We expect significantly improved capabilities to be in place for the next solar cycle, when our society will be even more susceptible to the negative impacts of space weather. NRL is leading the way in research efforts in this field.

## ACKNOWLEDGMENTS

The author acknowledges assistance from staff in the NRL Solar Physics branch in preparing this article, particularly Angelos Vourlidas, Dennis Socker, and Russell Howard. Assistance and advice from Daniel Wilkinson and Bill Murtagh at the NOAA SEC are also appreciated. The graphics were prepared by Mary Helen Gregory at Praxis, Inc. in Alexandria, VA. This work was carried out under NASA DPR S-13813-G.

## References

- <sup>1</sup> P. Song, H.J. Singer, and G.L. Siscoe, eds., "Space Weather," *Geophysical Monograph* **125**, American Geophysical Union, Washington, DC, 2001.
- <sup>2</sup> B. Fleck, V. Domingo, and A.I. Poland, ed., "The SOHO Mission," *Solar Physics* **162** (1-2), (1995). ★